Studying the effect of the gravity of the base plate by the chain on the pair of shafts

Cite as: AIP Conference Proceedings **2612**, 050039 (2023); https://doi.org/10.1063/5.0113270
Published Online: 15 March 2023

T. Z. Sultanov, G. A. Bahadirov, Z. A. Rakhimova, et al.

Studying the Effect of the Gravity of the Base Plate by the Chain on the Pair of Shafts

T. Z. Sultanov[1], G. A. Bahadirov[2], Z. A. Rakhimova[3] and E. S. Toshmatov[1, a)]

[1]*Tashkent Institute of Irrigation and Agricultural Mechanization Engineers, 100000, Tashkent, Uzbekistan*
[2]*Institute of Mechanics and Seismic Stability of Structures of the Academy of Sciences of the Republic of Uzbekistan, 100125, Tashkent, Uzbekistan*
[3]*Tashkent chemical – technological Institute, 100011, Tashkent, Uzbekistan*

[a)] Corresponding author: t.elyor85@mail.ru

Abstract. In this paper, in a vertical shaft machine machining flat material, the flat material base plate exits the coverage area of the first elastic-coated working shaft pair and hits the coverage area of the second elastic-coated working shaft pair, taking into account how the forces acting on the shaft change resistance moment and how the values of the force pulling the base plate upwards by the chain change relative to other quantities are investigated.

INTRODUCTION

The leather industry includes many technological machines; The machine with squeezing rollers is used in many operations, for example, during wringing, degreasing and after dyeing leather semi-finished products in a drum. The article presents the results of experimental studies to determine the effect of multilayer wet leather semi-finished products with monsoons during pressing on the amount of extracted moisture. Mathematical dependences of the amount of extracted moisture for each layer of a five-layer wet leather semi-finished product on the feed rate between the pressure rollers and the pressure of the rollers have been obtained [1]–[5].

When rolling and cooling on stand-coolers, the profiles receive general and local curvatures to correct which straightening on roller levelers (RLM) is used. Calculating the leveling parameters of bars on the RLM is based on the hypothesis of isotropy and uniformity of the deformed metal. In addition, the calculation is also based on the assumptions about the linear distribution of the coefficient of penetration of plastic deformation over the thickness of the rolled product with alternating bending, the point nature of the contact between the roller and the rolled surface, and the vertical direction of the leveling force for all RLM rollers. The use of these hypotheses significantly reduces the accuracy of calculating technological parameters during rolling and straightening. A mathematical model of the parameters of the alignment of profile bars in the calculation of RLM is presented [6].

While contributing significantly to the country's economic growth and stability, the leather industry does not have a good image because of its role in environmental pollution. This study will help managers of tanneries formulate strategies for the optimal use of available resources and waste reduction in the context of a circular economy [7].

The article examines the construction of automatic lines connecting several operations for the processing of leather semi-finished products. These automatic lines are believed to provide improved product quality and production efficiency. In addition, the kinematics of the cutter shaft is another area of research. A conveyor is proposed that ensures the stable operation of automatic lines for processing leather semi-finished products, and its efficiency is checked. The results obtained indicate that without stopping the technological cycle of sheet material processing, the stable operation of the automatic line is ensured. When obtaining the results, mathematical modeling was chosen as the key method, and to obtain the results; an MS Excel spreadsheet is used [8].

The Third International Scientific Conference Construction Mechanics, Hydraulics and Water Resources Engineering (CONMECHYDRO 2021 AS)
AIP Conf. Proc. 2612, 050039-1–050039-9; https://doi.org/10.1063/5.0113270
Published by AIP Publishing. 978-0-7354-4337-2/$30.00

In this case, the equations of motion of common pairs of machines for machining in the vertical and horizontal directions to a flat material using the equations of motion of the 2nd Lagrange circle are derived from the generalized coordinates for a single case. Also, based on the solutions of the extracted equations, graphs were constructed and analyzed for various parameters of the shaft pairs [9], [10]. The results of the study of normal stresses in two-roll modules are presented. An asymmetric two-roll module is considered; when the rolls are inclined to the right relative to the vertical, the diameters of the rolls are not the same, the rolls have elastic coatings with different rigidity, the material layer is fed down. Mathematical models of the distribution of normal stresses in the considered two-roll module in the case when the deformation properties of the contacting bodies are set by theologically determined models [11]. A mathematical method for computerized calculation of tension in 380 wires in the unwinding zone and behind the guide/input rollers on a titration machine is presented [12]. New analytical dynamic models have been developed for roller machines used in industry [13], [14].

For nonholonomic systems of mechanical systems, the equations of motion are derived and analyzed [15], [16]. In this work [17]–[23], the problem of choosing the appearance of the orientational surface with the uniform transfer of a smooth material to the processing zone of flat material is considered and investigated, i.e. between the working shafts. The movement of flat material in the processing zone along the conveyor has been investigated. The laws of dynamics and numerical methods were used to determine the appearance of the transfer surface.

MATERIALS AND METHODS

On the one hand, the construction of a line for transportation and mechanical processing of flat material, i.e. leather semi-finished products, was developed. This technological line has three main working zones, where various technological processes are carried out using pairs of working shafts and base plates. In the case under consideration, we consider the following issue for a vertical roller machine that mechanically processes flat material to operate at the required level. To do this, the following process is performed below, taking into account the moment of resistance of the base plate on which the flat material is suspended from the coverage area of the first elastic-coated working shaft pairs and how the forces acting on the shafts change when the second elastic-coated working pair strikes the coverage area (Figure 1). we analyze how the values of the force pulling the plate up change relative to other quantities.

To do this, we perform this process below; namely, the flat material researched base plate using Lagrange's 1-round equations for the condition of the first elastic-coated working Shaft pairs going out of the coverage zone and hitting the second elastic-coated working Val pairs going into the coverage zone (Figure 2), creating equations concerning the sizes we need. First, we determine the degree of freedom of the system under consideration (according to Figure 1). In this case, the degree of freedom, in this case, is three because the pairs of shafts covered with elastic material move in a straight parallel at the exit of the base plate from the coverage area. Since the base plate is in forwarding motion along the chain, the degree of freedom, in this case, is two-fold. When the base plate hits a pair of shafts lined with a high working elastic material, the shafts are in rotational motion, in which case the degree of freedom is one. This means that the degree of freedom of the system we are looking at is six. But assuming that there are four links to the system we are looking at, we assume that the degree of freedom of our system is equal to two. The generalized coordinates will also be two. These are as follows: $\psi = q_1, \varphi = q_2$.

We can construct the equations of motion for the case where the base plate on which the flat material is suspended leaves the coverage area of the first working elastic-coated shaft pair and hits the coverage area of the second working shaft pair. To do this, we calculate the kinetic energy of the avallo base plate and the elastic-coated shafts.

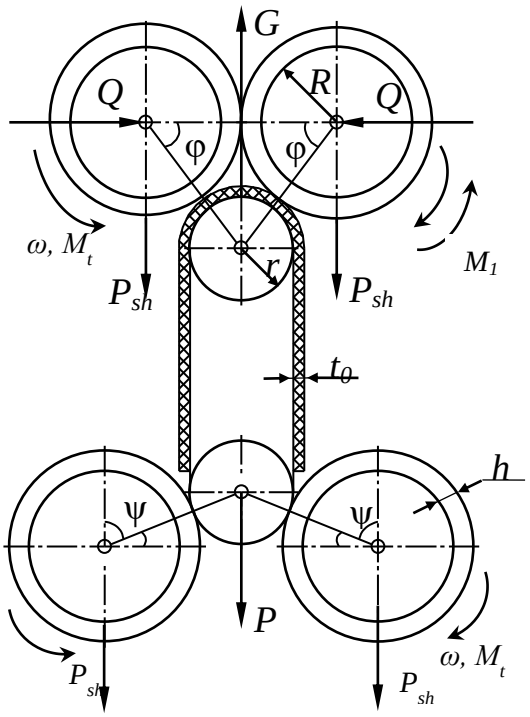

FIGURE 1. Diagram of the base plate exiting the coverage area of the first elastic-coated working shaft pairs and hitting the second elastic-coated working shaft pairs in the coverage area

In this case, the base plate on which the flat material is suspended moves forward throughout the system, and its kinetic energy is expressed as follows.

$$T_1 = \frac{M\vartheta_c^2}{2} = \frac{1}{2} m_1 \dot{y}^2, \tag{1}$$

where $T_1 -$is the kinetic energy of the base plate, $m_1 -$ is the mass of the chain, base plate and flat material.

The pair of bottom shafts in question moves in a straight parallel at the exit from the coverage area of the base plate on which the flat material is hung (Figure 1), and their kinetic energy is written as follows:

$$T_2 = T_3 = \frac{M\vartheta_c^2}{2} + I_{Cz}\frac{\omega^2}{2} = \frac{1}{2} m\dot{x}^2 + \frac{1}{2} J_x \omega^2, \tag{2}$$

where T_2, T_3 are the kinetic energy of the lower shafts, $m = m_2 = m_3$ is the mass of the lower shafts, J_{Cz} is the moment of inertia about the axis passing through the center of mass of the shaft perpendicular to the plane of motion, $\omega -$ angular velocity. The moment of inertia of the shaft is equal to $J_x = \frac{mR^2}{2}$ in question, where R is radius of shafts.

When the base plate on which the flat material is hung hits the coverage area of the second working elastic-coated shafts above, the shafts move in a slow rotational motion. In this case, the kinetic energy of the above shafts is expressed as follows:

$$T_4 = T_5 = I_z \frac{\omega^2}{2} \tag{3}$$

Where $T_4, T_5 -$ are the kinetic energy of the upper shafts. $m = m_4 = m_5 -$ is the mass of the upper shafts. $J_z -$ is moment of inertia about the axis of rotation of the shaft, $\omega -$ is angular velocity. In this case, the moment of inertia of the shaft with respect to the axis of rotation is equal to. $J_x = \frac{3mR^2}{2}$ according to the Huygens-Steiner theorem. Where $R -$ is radius of shafts.

Now we connect the *x* and *y* coordinates with the angle of coverage ψ for the lower shafts, in which case we have the following expression:

$$\begin{aligned} x &= (R + r + h_0)\cos\psi, \\ y &= (R + r + h_0)\sin\psi, \end{aligned} \tag{4}$$

where $R -$ is the radius of shafts, $r -$ is the radius of the "nose" of the base plate, $h_0 -$ is the thickness of the elastic coating of the shafts. If we derive the expression from (4), it is equal to the following.

$$\begin{aligned} \dot{x} &= -(R + r + h_0)\dot{\psi}\sin\psi, \\ \dot{y} &= (R + r + h_0)\dot{\psi}\cos\psi. \end{aligned} \tag{5}$$

Now we connect the *x* and *y* coordinates with the coverage angle for the upper shaft pairs, in which case we have the following expression:

$$\begin{aligned} x &= (R + r + h_0 + t_0)\cos\varphi, \\ y &= (R + r + h_0 + t_0)\sin\varphi, \end{aligned} \tag{6}$$

where $R -$ is the radius of shafts, $r -$ is the radius of the "nose" of the base plate, $h_0 -$ is elastic coating thickness of shafts, $t_0 -$ is the initial thickness of the flat material. If we derive the expression from (6), it is equal to the following.

$$\begin{aligned} \dot{x} &= -(R + r + h_0 + t_0)\dot{\varphi}\sin\varphi, \\ \dot{y} &= (R + r + h_0 + t_0)\dot{\varphi}\cos\varphi. \end{aligned} \tag{7}$$

To construct the differential equation of motion of a pair of elastic-coated shafts, we use Lagrange's second-order equation of motion.

$$\frac{d}{dt}\frac{\partial T}{\partial \dot{q}_i} - \frac{\partial T}{\partial q_i} = Q_i \qquad \text{(i=1,2)} \tag{8}$$

That is, we have the following two equations.

$$\frac{d}{dt}\frac{\partial T}{\partial \dot{\psi}} - \frac{\partial T}{\partial \psi} = Q_\psi \tag{9}$$

$$\frac{d}{dt}\frac{\partial T}{\partial \dot{\varphi}} - \frac{\partial T}{\partial \varphi} = Q_\varphi. \tag{10}$$

where $Q_i -$ is generalized forces.

Now we calculate the total kinetic energy. To do this, we can write the total kinetic energy for the lower shaft pairs, taking into account the sum of expressions (1) and (2) and expression (4), as follows:

$$T = T_1 + T_2 + T_3 = \frac{1}{2} m_1 \dot{y}^2 + 2\left(\frac{1}{2} m\dot{x}^2 + \frac{1}{2} J_{Cz}\omega^2\right)^2 = \frac{1}{2} m_1 (R + r + h_0)^2 \dot{\psi}^2 \cos^2\psi + \\ + m(R + r + h_0)^2 \dot{\psi}^2 \sin^2\psi + \frac{m_2 R^2}{2}\dot{\psi}^2 \tag{11}$$

Given the sum of expressions (1) and (3) and expression (6), we can write the total kinetic energy for the upper shaft pairs as follows:

$$T = T_1 + T_4 + T_5 = \frac{1}{2} m_1 \dot{y}^2 + 2\left(I_z \frac{\omega^2}{2}\right) = \frac{1}{2} m_1 (R + r + h_0 + t_0)^2 \dot{\varphi}^2 \cos^2\varphi + \frac{3mR^2}{2}\dot{\varphi}^2 \tag{12}$$

For lower shaft pairs, we calculate the total and specific derivatives of the kinetic energy.

$$\frac{\partial T}{\partial \dot{\psi}} = m_1 (R + r + h_0)^2 \dot{\psi}\cos^2\psi + 2m(R + r + h_0)^2 \dot{\psi}\sin^2\psi + mR^2\dot{\psi}, \tag{13}$$

$$\frac{d}{dt}\frac{\partial T}{\partial \dot{\psi}} = m_1 (R + r + h_0)^2 \ddot{\psi}\cos^2\psi - 2m_1 (R + r + h_0)^2 \dot{\psi}\sin\psi\cos\psi + 2m(R + r + h_0)^2 \ddot{\psi}\sin^2\psi + \\ + 4m(R + r + h_0)^2 \dot{\psi}\sin\psi\cos\psi + mR^2\ddot{\psi} \tag{14}$$

$$\frac{\partial T}{\partial \psi} = -m_1 (R + r + h_0)^2 \dot{\psi}^2 \sin\psi\cos\psi + 2m(R + r + h_0)^2 \dot{\psi}^2 \sin\psi\cos\psi \tag{15}$$

Firstly, we find the work done by calculating the angular displacement of the generalized forces ψ for the lower shaft pairs.

$$\delta A_\psi = Q_\psi \delta\psi\ , \tag{16}$$

$$\delta A_\psi = -2M_t\delta\psi + M_1\delta\psi - 2Q\delta x - P\delta y + 2P_{sh}\delta y + G\delta y\ , \tag{17}$$

where $G-$ is gravitational force acting on the base plate by the chain, $P-$ is chain, base plate and gravity of flat material, $P_в -$ is gravity of shafts, $Q = Q_2 = Q_3 -$ is pressure force acting on the shafts, $M_t -$ is rotating torque, $M_1 -$ is resistance torque.

(17) the δx and δy shifts in the expression are as follows:

$$\delta x = -(R + r + h_0)\sin\psi\delta\psi \\ \delta y = (R + r + h_0)\cos\psi\delta\psi, \tag{18}$$

If we put the expressions in equation (18) into equation (17), the expression looks like this:

$$\delta A_\psi = -2M_t\delta\psi + 2M_1\delta\psi + 2Q(R + r + h_0)\sin\psi\delta\psi + +(2P_{sh} - P + G)(R + r + h_0)\cos\psi\delta\psi \tag{19}$$

From Equation (19) we determine the generalized force Q_ψ

$$Q_{\psi} = -2M_{вр} + 2M_1 + 2Q(R + r + h_0)\sin\psi + (2P_в - P + G)(R + r + h_0)\cos\psi \quad (20)$$

Substituting the expressions (13) - (15) and (20) into the second-order equations of Lagrange (9), we obtain the equations of motion for the lower shaft pairs.

$$\begin{aligned} &m_1(R + r + h_0)^2\ddot{\psi}\cos^2\psi - 2m_1(R + r + h_0)^2\dot{\psi}\sin\psi\cos\psi + 2m(R + r + h_0)^2\ddot{\psi}\sin^2\psi + \\ &+ 4m(R + r + h_0)^2\dot{\psi}\sin\psi\cos\psi + mR^2\ddot{\psi} + m_1(R + r + h_0)^2\dot{\psi}^2\sin\psi\cos\psi + 2m(R + r + h_0)^2\dot{\psi}^2\sin\psi\cos\psi = \\ &= -2M_{вр} + 2M_1 + 2Q(R + r + h_0)\sin\psi + (2P_в - P + G)(R + r + h_0)\cos\psi \end{aligned} \quad (21)$$

It is known that since the base plate moves at a constant speed, the angular velocity of the shafts is $\omega = \dot{\psi}$ = const, and the angular acceleration is. In that case (21) for the lower shaft pairs, the equation of motion is as follows:

$$\begin{aligned} &((4m - 2m_1) + (m_1 + m))(R + r + h_0)^2\omega\sin\psi\cos\psi = \\ &= -2M_{вр} + 2M_1 + (2Q\sin\psi + (2P_в - P + G)\cos\psi)(R + r + h_0) \end{aligned} \quad (22)$$

(22) simplifying the equation leads to this appearance:

$$\frac{1}{2}((4m - 2m_1) + (m_1 + m))(R + r + h_0)^2\omega\sin 2\psi - (2Q\sin\psi + (2P_в - P + G)\cos\psi)(R + r + h_0) + 2M_{вр} - 2M_1 = 0 \quad (23)$$

(23) we can see from the equation that is a quadratic equation with respect to $(R + r + h_0)$.

$$a(R + r + h_0)^2 + b(R + r + h_0) + c = 0 \quad (24)$$

Where $a = \frac{1}{2}((4m - 2m_1) + (m_1 + m))\sin 2\psi\omega$, $b = -(2Q\sin\psi + (G - P + 2P_в)\cos\psi$, $c = 2(M_{вр} - M_1)$
(24) the solution of the quadratic equation can be written as follows.

$$R_{1,2} = \frac{-b \pm \sqrt{b^2 - 4ac}}{2a} - (r + h_0). \quad (25)$$

For high shaft pairs, we calculate the total and specific derivatives of the kinetic energy.

$$\frac{\partial T}{\partial\dot{\varphi}} = m_1(R + r + h_0 + t_0)^2\dot{\varphi}\cos^2\varphi + 3m_4R^2\dot{\varphi}, \quad (26)$$

$$\frac{\partial T}{\partial\varphi} = -m_1(R + r + h_0 + t_0)^2\dot{\varphi}^2\sin\varphi\cos\varphi, \quad (27)$$

$$\frac{d}{dt}\frac{\partial T}{\partial\dot{\varphi}} = m_1(R + r + h_0 + t_0)^2\ddot{\varphi}\cos^2\varphi - 2m_1(R + r + h_0 + t_0)^2\dot{\varphi}\sin\varphi\cos\varphi + 3mR^2\ddot{\varphi}, \quad (28)$$

We find the work done for upper shaft pairs by calculating the generalized forces at an angle, giving a displacement.

$$\delta A_{\varphi} = Q_{\varphi}\delta\varphi, \quad (29)$$

$$\delta A_{\varphi} = -2M_{вр}\delta\varphi + 2M_1\delta\varphi + 2Q\delta x - P\delta y + 2P_в\delta y + G\delta y, \quad (30)$$

(30) the displacements δx and δy in the expression are equal to the following for the upper shaft pairs.

$$\begin{aligned} \delta x &= -(R + r + h_0 + t_0)\sin\varphi\delta\varphi, \\ \delta y &= (R + r + h_0 + t_0)\cos\varphi\delta\varphi. \end{aligned} \tag{31}$$

If we put the expressions in equation (31) into equation (30), the expression looks like this.

$$\delta A_\varphi = -2M_{вр}\delta\varphi + 2M_1\delta\varphi - 2Q(R + r + h_0 + t_0)\sin\varphi\delta\varphi + (2P_в - P + G)(R + r + h_0 + t_0)\cos\varphi\delta\varphi \tag{32}$$

From Equation (32), we determine the generalized force Q_φ.

$$Q_\varphi = -2M_{вр} + 2M_1 - 2Q(R + r + h_0 + t_0)\sin\varphi + (2P_в - P + G)(R + r + h_0 + t_0)\cos\varphi \tag{33}$$

Substituting the defined expressions (26) - (28) and (33) into the second-round equations of (10) Lagrange, we derive the equations of motion for the upper shaft pairs.

$$\begin{aligned} &m_1(R + r + h_0 + t_0)^2\ddot{\varphi}\cos^2\varphi - 2m_1(R + r + h_0 + t_0)^2\dot{\varphi}\sin\varphi\cos\varphi + 3mR^2\ddot{\varphi} + m_1(R + r + h_0 + t_0)^2\dot{\varphi}^2\sin\varphi\cos\varphi = \\ &= -2M_{вр} + 2M_1 - 2Q(R + r + h_0 + t_0)\sin\varphi + (2P_в - P + G)(R + r + h_0 + t_0)\cos\varphi \end{aligned} \tag{34}$$

It is known that since the base plate moves at a constant speed, the angular velocity of the shafts is $\omega = \dot{\psi} =$ const, and the angular acceleration is $\varepsilon = 0$. In that case (34), the equation of motion for the upper shaft pairs is as follows:

$$\begin{aligned} &m_1(R + r + h_0 + t_0)^2\dot{\varphi}\sin 2\varphi - \frac{1}{2}m_1(R + r + h_0 + t_0)^2\dot{\varphi}^2\sin 2\varphi - 2M + 2M_1 + \\ &-(2Q\sin\varphi + (2P_в - P + G)\cos\varphi)(R + r + h_0 + t_0) = 0 \end{aligned} \tag{35}$$

If we simplify Equation (35), we get this view:

$$\left(1 - \frac{1}{2}\omega\right)m_1(R + r + h_0 + t_0)^2\omega\sin 2\varphi - (2Q\sin\varphi + (2P_в - P + G)\cos\varphi)(R + r + h_0 + t_0) - 2M_{вр} + 2M_1 = 0 \tag{36}$$

From equation (36), we can see that $(R + r + t_0 + h_0)$ is a relatively quadratic equation.

$$a(R + r + t_0 + h_0)^2 + b(R + r + t_0 + h_0) + c = 0 \tag{37}$$

Where $a = (1 - \frac{1}{2}\omega)m_1\sin 2\varphi\omega$, $b = -(2Q\sin\varphi + (G - P + 2P_в)\cos\varphi$, $c = 2(M_1 - M_{вр})$

The solution of the quadratic equation (37) can be written as follows.

$$R_{1,2} = \frac{-b \pm \sqrt{b^2 - 4ac}}{2a} - (r + t_0 + h_0). \tag{38}$$

RESULTS AND DISCUSSION

Based on the solutions of quadratic equations (25) and (35) given in the research process, graphs of radius dependence of the coverage angle of the lower and upper elastic coated shaft pairs were constructed and analyzed. In Figure 2, a graph of the radius dependence of the coverage angle of elastically coated shafts is constructed at different numerical values of the tensile force (for the position of the base plate lower shaft pairs at the exit from the coverage area). The graph shows that as the numerical values of the shaft coverage angle increase, the numerical values of the shaft radius decrease. Analyzing the graph, we can say that the smaller the numerical values of the gravitational force, the larger the numerical values of the radius of the shafts. In Figure 3, a graph of the radius dependence of the coverage angle of elastic-coated shafts is constructed at different numerical values of the tensile force (for the base plate's position when the upper shaft pairs hit the coverage area). As we can see from the graph, when the shafts' radius is large, the coverage angle is small, and when the radius of the shafts is small, the coverage angle reaches a large value.

CONCLUSION

As we examine how the traction force acting on the base plate from the chain side concerning other parameters depends on the parameters of the chain in the event that the flat material is tested, the first elastic-coated working shaft pair exits the coverage area, and the second elastic-coated working shaft pair hits the coverage area. Based on the theory we have written, we have come to the following conclusions.

Based on the constructed graphs, we can say that the larger the diameter of the shafts, the smaller the value of the force pulling the base plate upwards. Conversely, if the diameter of the shafts is small, the value of the force pulling the base plate upwards must be large. Based on the above conclusions, we can say that the numerical value of the traction force should be determined depending on the diameter of the selected shafts when the base plate exits the coverage area of the lower shaft pairs because the traction force must pull the base plate out of the coverage area at a constant speed. Because in this case, if a large gravitational force suddenly pulls up the base plate, the chain will break, and the constant speed of the base plate along the chain will not be ensured.

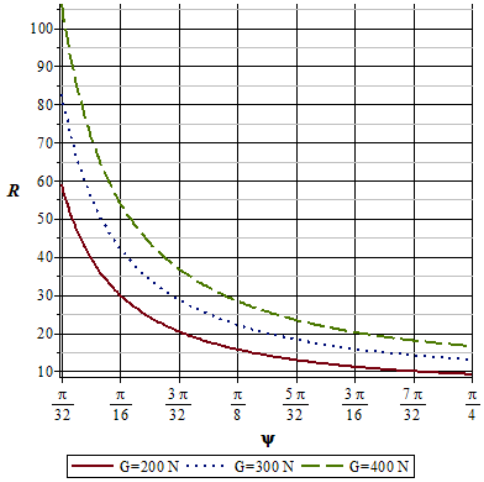

FIGURE 2. Graph of radius dependence of coverage angle of elastic coated shafts. (for the position of the bottom plate pairs of the base plate at the exit from the coverage area)

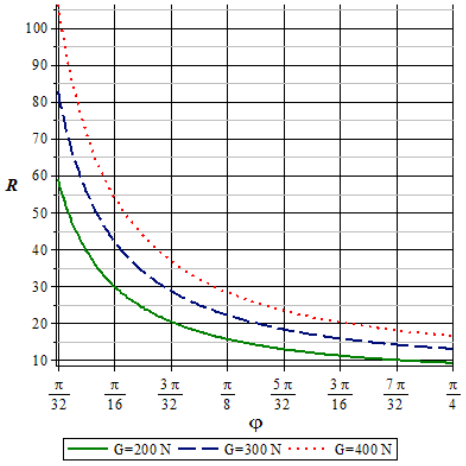

FIGURE 3. Graph of radius dependence of coverage angle of elastic coated shafts. (for the position of the base plate when the upper shaft pairs hit the coverage area)

REFERENCES

1. G. Bahadirov, G. Tsoy, and A. Nabiev, “STUDY OF THE EFFICIENCY OF SQUEEZING MOISTURE-SATURATED PRODUCTS,” *EUREKA Phys. Eng.*, (2021), doi: 10.21303/2461-4262.2021.001606.
2. A. M. Amanov, Auezhan T., Bahadirov, Gayrat A., Tsoy, Gerasim N., Nabiev, “A New Method to Wring Water-Saturated Fibrous Materials,” *Int. J. Mech. Eng. Robot. Res.*, vol. **10**, no. 3, pp. 151–156, (2021), doi: 10.18178/ijmerr.10.3.151-156.
3. A. Amanov, G. Bahadirov, T. Amanov, G. Tsoy, and A. Nabiev, “Determination of strain properties of the leather semi-finished product and moisture-removing materials of compression rolls,” *Materials (Basel).*, (2019), doi: 10.3390/ma12213620.
4. A. Bahadirov, G., Tsoy, G., Nabiev, A., Umarov, “Experiments on Moisture Squeezing from a Leather Semi-Finished Product,” *Int. J. Recent Technol. Eng.*, (2020), doi: 10.35940/ijrte.e6125.018520.
5. G. A. Bakhadirov, A. M. Nabiev, and A. A. Umarov, “Investigation of the process of squeezing a wet leather semi-finished product between a roller pair,” vol. **6**, no. 7, pp. 10240–10246, (2019).
6. A. Djuraev and A. Jumaev, “Providing the development of new designs for the design of the roller mechanism transmitting rotational motion in belt conveyors,” *Int. J. Emerg. Trends Eng. Res.*, (2020), doi: 10.30534/ijeter/2020/267892020.
7. G. A. Bahadirov, T. Z. Sultanov, and A. Abdukarimov, “Comparative analysis of two gear-lever differential inter-roller transmission mechanisms,” in *IOP Conference Series: Earth and Environmental Science*, (2020), doi: 10.1088/1755-1315/614/1/012102.
8. S. R. Khurramov, “Simulation of the form of contact curves rolls in two-roll modules,” in *IOP Conference Series: Earth and Environmental Science*, (2020), doi: 10.1088/1755-1315/614/1/012096.
9. G. A. Bahadirov and Z. A. Rakhimova, “Research the Position of the Base Plate is Located at a Distance from the Axes of the Working Elastic Covering Shafts,” *Int. J. Adv. Res. Sci. Eng. Technol.*, vol. **7**, no. 11, pp. 15845–15851, (2020).
10. G. Bahadirov and Z. Rakhimova, “Dynamics of Roler Pairs of Mechanical Processing Machine for Flat Material,” *Solid State Technol.*, vol. **64**, no. 2, pp. 2000–2010, (2021).
11. S. R. Khurramov and F. S. Khalturaev, “Simulation of contact voltages in two-roll modules,” in *IOP Conference Series: Earth and Environmental Science*, (2020), vol. **614**, no. 1,
12. S. R. Khurramov, “Some questions of the contact interaction theory in two-roll modules,” in *Journal of Physics: Conference Series*, (2020), doi: 10.1088/1742-6596/1546/1/012132.
13. J. Liu, “A dynamic modelling method of a rotor-roller bearing-housing system with a localized fault including the additional excitation zone,” *J. Sound Vib.*, (2020), doi: 10.1016/j.jsv.2019.115144.
14. J. Liu, L. Luo, Y. Hu, F. Wang, X. Zheng, and K. Tang, “Kinetics and mechanism of thermal degradation of vegetable-tanned leather fiber,” *J. Leather Sci. Eng.*, (2019), doi: 10.1186/s42825-019-0010-z.
15. K. Khusanov, “Stabilization of mechanical system with holonomic servo constraints,” in *IOP Conference Series: Materials Science and Engineering*, (2020), doi: 10.1088/1757-899X/883/1/012146.
16. K. Khusanov, “Stabilization of mechanical systems with nonholonomic servoconstraints,” in *IOP Conference Series: Materials Science and Engineering*, (2020), doi: 10.1088/1757-899X/883/1/012164.
17. K. Bahadirov, G., Musirov, M., Bakhadirov, “Parameters Substantiation of Guide Surface of Flat Material into the Processing Area,” *Int. J. Eng. Adv. Technol.*, vol. **9**, no. 4, (2020), doi: 10.35940/ijeat.d7655.049420.
18. N. A. M. Amanov T.YU., Baubekov S.D., Tsoy G.N., “Device To Ensure The Pressure Force Between The Working,” Mashin, Tekhnologicheskikh, no. **9**, pp. 9–14, (2018).
19. M. N. Zakharov and M. S. Kuts, “The approach to determine the elastic characteristic of the contact of rough surfaces,” *Int. J. Mech. Eng. Robot. Res.*, (2020), doi: 10.18178/ijmerr.9.7.937-942.
20. T. Mavlonov, A. Akhmedov, R. Saidakhmedov, and K. Bakhadirov, “Simulation modelling of cold rolled metal strip by asymmetric technology,” in *IOP Conference Series: Materials Science and Engineering*, (2020),
21. E.Toshmatov, A. Akhmedov, Z. Ibragimova, “Thermodynamic bases of mechanical working of metals by cutting”, *in IOP Conf. Series: Materials Science and Engineering.* (2020). **883**. Pp. 1–13.
22. G. Bahadirov, T. Sultanov, B. Umarov, and K. Bakhadirov, "Advanced machine for sorting potatoes tubers," (2020), doi: 10.1088/1757-899X/883/1/012132.
23. G.Bahadirov, Sh.Ravutov, A. Abdukarimov and E.Toshmatov, “Development of the methods of kinematic analysis of elliptic drum of vertical-spindle cotton harvester”, *in IOP Conf. Series: Materials Science and Engineering*. **1030** (2021) 012160. doi:10.1088/1757-899X/1030/1/012160.